Synthesis and Properties of New Aromatic Polyamides with Redox-Active 2,4-Dimethoxytriphenylamine Moieties

SHENG-HUEI HSIAO,[1] GUEY-SHENG LIOU,[2] YI-CHUN KUNG,[3] TZU-JUNG HSIUNG[3]

[1]Department of Chemical Engineering and Biotechnology, National Taipei University of Technology, Taipei 10618, Taiwan

[2]Institute of Polymer Science and Engineering, National Taiwan University, Taipei 10617, Taiwan

[3]Department of Chemical Engineering, Tatung University, Taipei 10451, Taiwan

Received 14 April 2010; accepted 8 May 2010
DOI: 10.1002/pola.24124
Published online in Wiley InterScience (www.interscience.wiley.com).

ABSTRACT: A new triphenylamine-based diamine monomer, 4,4′-diamino-2″,4″-dimethoxytriphenylamine (**2**), was synthesized from readily available reagents and was reacted with various aromatic dicarboxylic acids to produce a series of aromatic polyamides (**4a–h**) containing the redox-active 2,4-dimethoxy-substituted triphenylamine (dimethoxyTPA) unit. All the resulting polyamides were readily soluble in polar organic solvents and could be solution cast into tough and flexible films. These polymers exhibited good thermal stability with glass transition temperatures of 243–289 °C and softening temperatures of 238–280 °C, 10% weight loss temperatures in excess of 470 °C in nitrogen, and char yields higher than 60% at 800 °C in nitrogen. The redox behaviors of the polymers were examined using cyclic voltammetry (CV). All these polyamides showed two reversible oxidation processes in the first CV scan. The polymers also displayed low ionization potentials as a result of their dimethoxyTPA moieties. In addition, the polymers displayed excellent stability of electrochromic characteristics with coloration change from a colorless neutral state to green and blue-purple oxidized states. These anodically coloring polyamides showed high green coloration efficiency (CE = 329 cm^2/C), high contrast of optical transmittance change ($\Delta T\%$ = 84% at 829 nm), and long-term redox reversibility. © 2010 Wiley Periodicals, Inc. J Polym Sci Part A: Polym Chem 48: 3392–3401, 2010

KEYWORDS: cyclic voltammetry; electrochemistry; electrochromism; functionalization of polymers; polyamides; redox polymers; spectroelectrochemistry; triphenylamine

INTRODUCTION

Electrochromism consists in the formation of new optical transitions in an electroactive surface film or an electroactive solute as the result of electrochemical oxidation or reduction.[1] This is an intriguing phenomenon for which there might be a wide range of applications, including optical switching devices, smart windows, memory elements, large-area information panels, electronic papers (e-papers), and chameleon materials.[2–9] The earliest electrochromic materials in the visible region were the inorganic compounds such as tungsten trioxide (WO_3), iridium dioxide (IrO_2), and nickel oxides (NiO, Ni_2O_3).[10,11] Later, organic materials (i.e., viologens, metallophthalocyanines, and conjugated polymers) have received more attention than inorganics for electrochromic applications because of the different colors observed with these compounds while switching among their redox states.[12–15] Among the available organic electrochromic materials, π-conjugated polymers represented by polypyrrole and poly(3,4-ethylenedioxythiophene) (PEDOT) and their derivatives have received a great deal of attention because of their ease of processability, fast switching ability, high coloration efficiency and optical contrast ratio, long-term redox stability, and wide range of colors.[16–18]

Aromatic polyamides are well-known high-performance polymers with excellent mechanical and thermal properties.[19] However, rigidity of the backbone and strong interchain interactions result in high melting or glass transition temperatures (T_g) and limited solubility in most organic solvents. These properties make them generally intractable or difficult to process, thus restricting their wide-spread applications. To overcome such a difficulty, polymer structure modification becomes necessary. One of the common approaches for increasing solubility and processability of aromatic polyamides without sacrificing high thermal stability is the introduction of bulky, packing-disruptive groups into the polymer backbone.[20,21] We have demonstrated that aromatic polyamides containing bulky, propeller-shaped triphenylamine (TPA) unit are amorphous, have good solubility in organic solvents, and exhibit high mechanical property and thermal stability.[22] In recent years, TPA-based high-performance polymers such as polyamides and polyimides with attractive electrochromic properties have been reported in this study and in the study by Liou et al.[23] The electrochromic function of these polymers originates from the electroactive TPA

Additional Supporting Information may be found in the online version of this article. Correspondence to: S.-H. Hsiao (E-mail: shhsiao@ntut.edu.tw)
Journal of Polymer Science: Part A: Polymer Chemistry, Vol. 48, 3392–3401 (2010)

moieties, which can reversibly be oxidized as long as the *para*-position of the phenyl rings is protected.

TPAs with substituents in their *para*-position generally show reversible one-electron oxidation behavior.[24] As demonstrated previously,[23(e)] polyamides on the basis of 4,4′-diamino-4″-methoxytriphenylamine exhibit excellent electrochemical and electrochromic stability, together with high coloration efficiency, high optical contrast, and fast switching speed. Inspired by the encouraging results, herein we synthesize 4,4′-diamino-2″,4″-dimethoxytriphenylamine (**2**) and its derived polyamides containing redox-active TPA units with electron-donating methoxy groups *para*- and *ortho*-substituted on the pendent phenyl ring. The polyamides described in this work exhibit comparable electrochemical and electrochromic stability in comparison with that of the corresponding polyamides with only one methoxy group *para*-substituted on the pendent phenyl ring of the TPA unit.[23(e)] Additionally, it is interesting to emphasize that the additional substitution of *ortho* methoxy group on the TPA unit gives the resulting polyamides another stable oxidized state; thus, two differently colored redox states of the polymers can be accessed through electrochemical oxidation.

EXPERIMENTAL

Materials

2,4-Dimethoxyaniline (Acros), 4-fluoronitrobenzene (Acros), hydrazine monohydrate (TCI), 10% palladium on charcoal (Pd/C) (Fluka), and cesium fluoride (CsF; Acros) were used as received. The aromatic dicarboxylic acids that include terephthalic acid (**3a**) (TCI), isophthalic acid (**3b**) (TCI), 4,4′-biphenyldicarboxylic acid (**3c**) (TCI), 4,4′-dicarboxydiphenyl ether (**3d**) (TCI), 4,4′-sulfonyldibenzoic acid (**3e**) (New Japan Chemical Co.), 2,2-bis(4-carboxyphenyl)-1,1,1,3,3,3-hexafluoropropane (**3f**) (TCI), 1,4-napthalenedicarboxylic acid (**3g**) (Wako), and 2,6-napthalenedicarboxylic acid (**3h**) (TCI) were used as received. Triphenyl phosphite (TPP; Acros) was purified by distillation under reduced pressure. Commercially obtained anhydrous calcium chloride ($CaCl_2$) was dried under vacuum at 180 °C for 8 h before use. Tetrabutylammonium perchlorate (TBAP; TCI) was recrystallized twice by ethyl acetate under nitrogen atmosphere and then dried *in vacuo* before use. Dimethyl sulfoxide (DMSO; Tedia), *N*,*N*-dimethylacetamide (DMAc; Tedia), *N*,*N*-dimethylformamide (DMF; Tedia), pyridine (Py; Wako), and *N*-methyl-2-pyrrolidone (NMP; Fluka) were dried over calcium hydride for 24 h, distilled under reduced pressure, and stored over 4 Å molecular sieves in a sealed bottle.

Monomer Synthesis

Synthesis of 4,4′-Dinitro-2″,4″-dimethoxytriphenylamine (1)

2,4-Dimethoxyaniline (15.32 g, 0.10 mol) and cesium fluoride (30.38 g, 0.20 mol) were dissolved in dimethyl sulfoxide (DMSO, 100 mL) in a 500-mL round-bottomed flask. Then, 4-fluoronitrobenzene (28.3 g, 0.20 mol) was added, and the reaction solution was heated at 120 °C for 18 h. The mixture was allowed to cool and poured into 1 L of MeOH/water (2:1) to precipitate orange-yellow crystals. The product was collected and dried to afford 31.2 g (yield 76%) of pure **1**; mp = 167–169 °C (by DSC, 10 °C/min). IR (KBr): 1579 cm^{-1}, 1338 cm^{-1} (—NO_2 stretch). ^{1}H-NMR (500 MHz, DMSO-d_6, δ, ppm) (for the peak assignments, see Supporting Information Fig. S2): 8.15 (d, J = 9.2 Hz, 4H, H_a), 7.23 (d, J = 8.6 Hz, 1H, H_c), 7.13 (d, J = 9.2 Hz, 4H, H_b), 6.79 (d, J = 2.6 Hz, 1H, H_e), 6.67 (dd, J = 8.6, 2.6 Hz, 1H, H_d), 3.83 (s, 3H, —OCH_3), 3.67 (s, 3H, —OCH_3). ^{13}C-NMR (125 MHz, DMSO-d_6, δ, ppm) (for the peak assignments, see Supporting Information Fig. S2): 160.44 (C^8), 156.57 (C^{10}), 151.41 (C^4), 141.42 (C^1), 130.90 (C^6), 125.33 (C^2), 124.53 (C^5), 120.56 (C^3), 106.42 (C^7), 100.4 (C^9), 55.89 (C^{11}), 55.49 (C^{12}).

Synthesis of 4,4′-Diamino-2″,4″-dimethoxytriphenylamine (2)

In a 500-mL round-bottom flask, a mixture of 10 g (0.03 mol) of dinitro compound **1**, 0.15 g of 10 wt % Pd/C, 10 mL of hydrazine monohydrate, and 150 mL of ethanol was heated at a reflux temperature for about 10 h. The resultant solution was filtered to remove the catalyst, and the filtrate was concentrated by rotary evaporation. The precipitate was collected and dried in vacuum to give 7.92 g (yield 62%) of pure 4,4′-diamino-2″,4″-dimethoxytriphenylamine (**2**) as pale-gray crystals; mp = 131–132 °C (by DSC, 10 °C/min). IR (KBr): 3219–3407 cm^{-1} (*N*—H stretch). Anal. Calcd for $C_{20}H_{21}N_3O_2$ (335.40): C, 71.62%; H, 6.31%; N, 12.53%. Found: C, 71.60%; H, 6.28%; N, 12.42%. ^{1}H-NMR (500 MHz, δ, ppm, DMSO-d_6) (for the peak assignments, see Fig. 1):

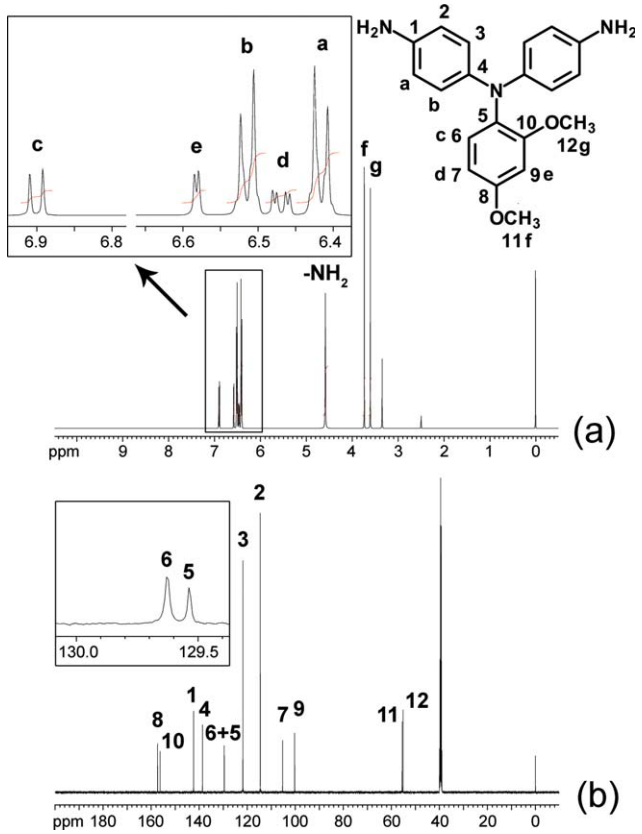

FIGURE 1 (a) ^{1}H-NMR and (b) ^{13}C-NMR spectra of the diamine monomer **2** in DMSO-d_6. [Color figure can be viewed in the online issue, which is available at www.interscience.wiley.com.]

6.90 (d, J = 8.6 Hz, 1H, H_c), 6.58 (d, J = 2.7 Hz, 1H, H_e), 6.51 (d, J = 8.7 Hz, 4H, H_b), 6.47 (dd, J = 8.7, 2.7 Hz, 1H, H_d), 6.41 (d, J = 8.7 Hz, 4H, H_a), 4.59 (s, 4H, —NH_2), 3.74 (s, 3H, —OCH_3), 3.60 (s, 3H, —OCH_3). ^{13}C-NMR (125 MHz, δ, ppm, DMSO-d_6) (for the peak assignments, see Fig. 1): 157.34 (C^8), 156.31 (C^{10}), 142.34 (C^1), 138.6 (C^4), 129.61 (C^6), 129.53 (C^5), 121.82 (C^3), 114.55 (C^2), 105.32 (C^7), 100.28 (C^9), 55.52 (C^{11}), 55.14 (C^{12}).

Synthesis of Polyamides

The synthesis of polyamide **4a** is used as an example to illustrate the general synthetic route used to produce the polyamides. A 50-mL round-bottom flask equipped with a magnetic stirrer was charged with 0.5031 g (1.50 mmol) of diamine momomer **2**, 0.2492 g (1.50 mmol) of terephthalic acid (**3a**), 1.5 mL of TPP, 2.5 mL of NMP, 0.8 mL of pyridine, and 0.15 g of calcium chloride ($CaCl_2$). The reaction mixture was heated with stirring at 110 °C for 3 h. The resulting polymer solution was poured slowly into 200 mL of stirring methanol giving rise to a stringy, fiber-like precipitate that was collected by filtration, washed thoroughly with hot water and methanol, and dried. IR (film): 3298 cm^{-1} (amide N—H stretch), 1653 cm^{-1} (amide C=O stretch).

Preparation of the Polyamide Films

A polymer solution was made by the dissolution of about 0.7 g of the polyamide sample in 10 mL of hot DMAc. The homogeneous solution was poured into a 9-cm glass Petri dish, which was placed in a 90 °C oven overnight for the slow release of the solvent, and then the film was stripped off from the glass substrate and further dried in vacuum at 160 °C for 6 h. The obtained films were about 0.09-mm thick and were used for X-ray diffraction measurements, solubility tests, and thermal analyses.

Measurements

Infrared (IR) spectra were recorded on a Horiba FT-720 FT-IR spectrometer. Elemental analyses were run in a Heraeus VarioEL III CHNS elemental analyzer. ^{1}H- and ^{13}C-NMR spectra were measured on a Bruker AVANCE 500 FT-NMR system with tetramethylsilane as an internal standard. The inherent viscosities were determined with a Cannon-Fenske viscometer at 30 °C. Wide-angle X-ray diffraction measurements were performed at room temperature (~25 °C) on a Shimadzu XRD-6000 X-ray diffractometer with a graphite monochromator (operating at 40 kV and 30 mA), using nickel-filtered Cu-Kα radiation (λ = 1.5418 Å). The scanning rate was 2°/min over a range of 2θ = 10°–40°. DSC analyses were performed on a Perkin–Elmer Pyris 1 DSC at a scan rate of 20 °C/min in flowing nitrogen. Thermogravimetric analysis (TGA) was performed with a Perkin–Elmer Pyris 1 TGA. Experiments were carried out on approximately 4–6 mg of samples heated in flowing nitrogen or air (flow rate = 40 cm^3/min) at a heating rate of 20 °C/min. Thermomechanical analysis (TMA) was determined with a Perkin–Elmer TMA 7 instrument. The TMA experiments were carried out from 50 to 350 °C at a scan rate of 10 °C/min with a penetration probe 1.0 mm in diameter under an applied constant load of 10 mN. Softening temperatures (T_s) were taken as the onset temperatures of probe displacement on the TMA traces. Ultraviolet–visible (UV–vis) spectra of the polymer films were recorded on a Jasco UV/VIS V530 spectrometer. Photoluminescence (PL) spectra were obtained on a Varian Cary Eclipse fluorescence spectrophotometer. Electrochemistry was performed with a CH Instruments 600C electrochemical analyzer. Voltammograms are presented with the positive potential pointing to the left and with increasing anodic currents pointing downward. Cyclic voltammetry (CV) was conducted with the use of a three-electrode cell in which ITO (polymer films area about 0.7 cm × 1.4 cm) was used as a working electrode. A platinum wire was used as an auxiliary electrode. All potentials were reported with respect to Ag/AgCl electrode at room temperature under a nitrogen atmosphere. Ferrocene was used as an external reference for calibration (+0.44 V vs. Ag/AgCl). An Agilent 8453 UV-Visible photodiode array spectrophotometer was used to conduct the spectroelectrochemical experiments. For the spectroelectrochemical studies, the polymer film cast on an ITO-coated glass slide was immersed in 0.1 M TBAP/MeCN solution using a UV-cuvette as a single-compartment cell equipped with a Pt counter electrode and a Ag/AgCl reference electrode.

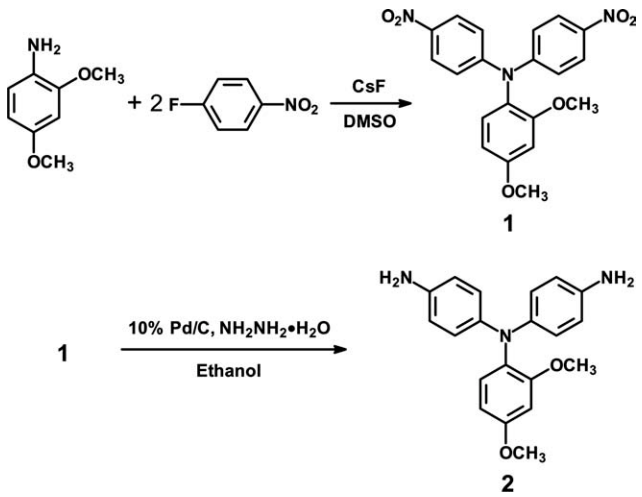

SCHEME 1 Synthetic route to the dimethoxyTPA-based diamine monomer **2**.

RESULTS AND DISCUSSION

Monomer Synthesis

According to a well-established synthetic method,[25] the target TPA-based diamine monomer, 4,4′-diamino-2″,4″-dimethoxytriphenylamine (**2**), was successfully synthesized by the CsF-mediated double N-arylation reactions of 2,4-dimethoxyaniline with two equivalent 4-fluoronitrobenzene, followed by catalytic reduction of the intermediate dinitro derivative **1** using Pd/C and hydrazine in refluxing ethanol (Scheme 1). The synthesized compounds **1** and **2** were fully characterized using elemental analysis and FTIR, ^{1}H-NMR, and ^{13}C-NMR spectroscopy. FTIR spectra of these two compounds are shown in Supporting Information Figure S1. The nitro

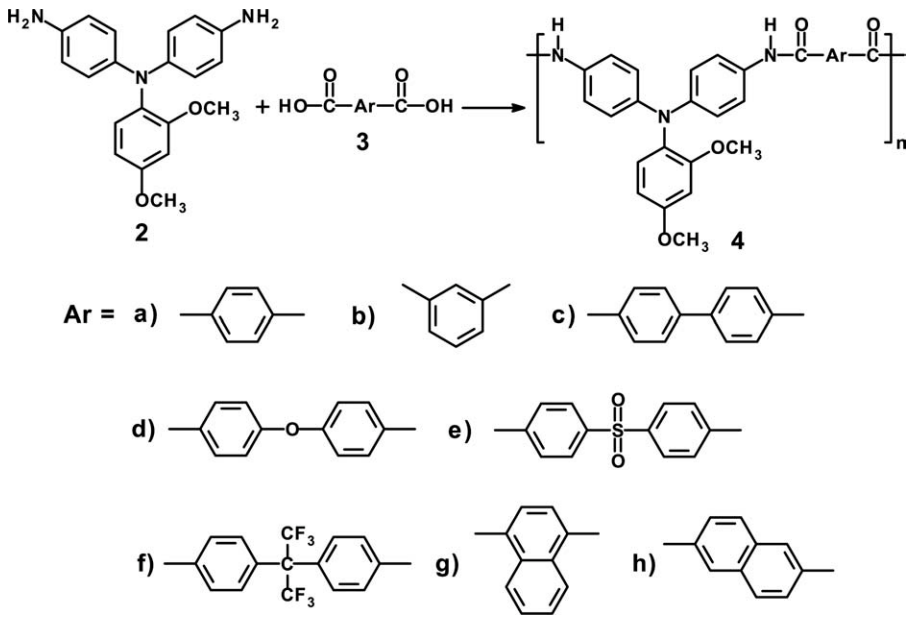

SCHEME 2 Synthesis of dimethoxy-TPA-based polyamides.

groups of compound **1** gave two characteristic bands at around 1579 and 1338 cm^{-1} (—NO_2 asymmetric and symmetric stretching). After reduction, the characteristic absorptions of the nitro group disappeared and the primary amino group showed the typical *N*—H stretching absorptions in the region of 3200–3400 cm^{-1}. The ^{1}H- and ^{13}C-NMR spectra of the dinitro derivative **1** are included in Supporting Information Figure S2. Figure 1 illustrates the ^{1}H- and ^{13}C-NMR spectra of the diamine monomer **2** in DMSO-d_6. The ^{1}H-NMR spectra clearly reveal that the nitro groups have been completely reduced to the amino groups by the high-field shift of the aromatic protons Ha and Hb and by the resonance signal at 4.6 ppm corresponding to the primary aromatic amino protons. Assignments of each proton and carbon atoms are assisted by the 2D NMR spectra as shown in Supporting Information Figure S3, and these spectra agree well with the proposed molecular structures of **1** and **2**.

Polymer Synthesis

According to the phosphorylation technique developed by Yamazaki et al.,[26] a series of novel TPA-based polyamides **4a–h**, with dimethoxy *ortho*- and *para*-substituted on the pendent phenyl ring, were prepared by the direct polycondensation reaction of diamine **2** with various aromatic dicarboxylic acids (**3a–h**) using triphenyl phosphite (TPP) and pyridine as condensing agents (Scheme 2). All the polymerizations proceeded homogeneously throughout the reaction and afforded clear, highly viscous polymer solutions. The polymers precipitated in a tough, fiber-like form when the resulting polymer solutions were slowly poured into stirred methanol. These polyamides were obtained in almost quantitative yields, with inherent viscosities in the range of 0.52–1.42 dL/g, as shown in Supporting Information Table S1. All the polymers can be solution cast into flexible and tough films, and this is indicative of the formation of high-molecular-weight polymers. Structural features of these polyamides were verified by FTIR spectroscopy. The FTIR spectra of these polymers showed characteristic amide absorptions around 3300 cm^{-1} (amide *N*—H stretching) and 1650 cm^{-1} (carbonyl C=O stretching).

Polymer Properties

Organo-Solubility and Film Morphology

The qualitative solubility properties of polyamides **4a–h** in several organic solvents at 10% (wt/vol) are summarized in Table S1. All polymers exhibited excellent solubility in a variety of solvents such as NMP, DMAc, DMF, DMSO, and *m*-cresol at room temperature. The high solubility can be attributed in part to the incorporation of packing-disruptive dimethoxyTPA groups, which retard dense chain packing and lead to a decreased chain–chain interaction. Therefore, these polymers have the advantage of allowing inexpensive solution processing techniques, such as spin-coating and printing methods, to be used for the preparation of large-area devices. All the polymers could afford flexible and tough films, and they were amorphous in nature as evidenced by wide-angle X-ray diffraction patterns. The mechanical property and amorphous nature of these polymers are important for the further development of flexible optoelectronic devices.

Thermal Properties

DSC, TMA, and TGA were used to investigate the thermal properties of all polyamides. The thermal behavior data of polyamides **4a–h** are summarized in Table 1. The polyamides showed high glass transition temperatures (T_gs) in the range of 243–289 °C by DSC. The T_g order corresponds to the decreasing order of stiffness and polarity of the polymer backbones. The relatively lower T_g values of polyamides **4b** and **4d** can be explained in terms of the flexibility and low rotation barrier of its diacid moiety. The highest T_g value of polyamide **4c** can be explained by the presence of rigid biphenylene unit in the diacid moiety that stiffens the polymer backbone.

TABLE 1 Thermal Properties of Polyamides

Polymer Code	T_g[a] (°C)	T_s[b] (°C)	T_d at 5 wt % Loss[c] (°C)		T_d at 10 wt % Loss[c] (°C)		Char Yield[d] (%)
			In N_2	In Air	In N_2	In Air	
4a	259	264	444	455	481	497	65
4b	243	238	437	437	472	483	68
4c	289	280	460	463	496	508	73
4d	254	252	443	439	480	482	68
4e	278	276	449	470	471	502	65
4f	277	269	455	494	500	549	61
4g	260	261	441	465	477	510	69
4h	263	269	439	481	473	530	71

[a] The samples were heated from 50 to 400 °C at a scan rate of 20 °C/min followed by rapid cooling to 50 °C at −200 °C/min in nitrogen. The midpoint temperature of baseline shift on the subsequent DSC trace (from 50 to 400 °C at heating rate 20 °C/min) was defined as T_g.
[b] Softening temperature measured by TMA using a penetration method.
[c] Decomposition temperature at which a 5% or 10% weight loss was recorded by TGA at a heating rate of 20 °C/min.
[d] Residual weight percentages at 800 °C under nitrogen flow.

The softening temperatures (T_s) of the polymer films were determined with TMA by the penetration method. The T_s value was read from the onset temperature of the probe displacement on the TMA curve. Figure 2 shows a typical TMA thermogram of polyamide **4e**. The T_s values of the **4** series polyamides are in the range from 238 to 280 °C. In most cases, the T_s values obtained by TMA are comparable to the T_g values measured by the DSC experiments.

The thermal stability of polyamides was evaluated by TGA in both air and nitrogen atmospheres. The Figure 2 inset depicts a typical set of TGA curves for polyamide **4e** in air and in nitrogen. The decomposition temperatures (T_d) at 5% and 10% weight losses in nitrogen and air atmosphere were taken from the original TGA thermograms and are given in Table 1. All the polymers exhibited good thermal stability; the T_ds of polyamides **4a–h** at a 10% weight loss were in the range of 471–500 °C in nitrogen and 482–549 °C in air. It is worthy to mention that in all cases, these polyamides revealed a delayed decomposition in air than in nitrogen. The reason is not clear at present. The amount of carbonized residues (char yield) at 800 °C in nitrogen for all polyamides was in the range of 61–73 wt %. The high char yields of these polyamides can be attributed to their high aromatic content. Thus, the thermal analysis results revealed that these polyamides exhibited excellent thermal stability, which in turn is beneficial to increase the service time in device application and enhance the morphological stability to the spin-coated film.

Optical and Electrochemical Properties

The optical properties of the dimethoxyTPA-based polyamides **4a–h** were investigated by UV–vis and photoluminescence (PL) spectroscopy, and the relevant data are presented in Table 2. These polymers exhibited strong UV–vis absorption bands at 278–382 nm in NMP solution, assignable to the π–π^* transitions resulting from the conjugated dimethoxyTPA segment. Their PL spectra in NMP solution showed emission maximum around 445–468 nm (in the blue region), with a very low fluorescence quantum yields of 0.33%–0.77%. The absorption spectra of the polyamides in the solid state are similar (a little red shifted) to those measured in NMP solution. Optical band gap (E_g) determined from the absorption edge of the solid-state spectra of polyamides are found to be 2.58–3.02 eV.

The electrochemical properties of these polyamides were investigated by cyclic voltammetry (CV) for the cast film on an ITO-coated glass substrate as working electrode in dry acetonitrile (MeCN) containing 0.1 M of TBAP as electrolyte salt under nitrogen atmosphere. One pair of reversible redox waves was observed in the first CV scan of these polymers. Figure 3 shows a representative CV curve for polyamide **4d** recorded at a scan rate of 50 mV/s. The CV diagram indicates two well-defined redox waves, with half-wave potentials ($E_{1/2}$) of 0.7 and 1.2 V. The first peak, at 0.82 V, can be ascribed to oxidation of the electron-rich nitrogen atom in

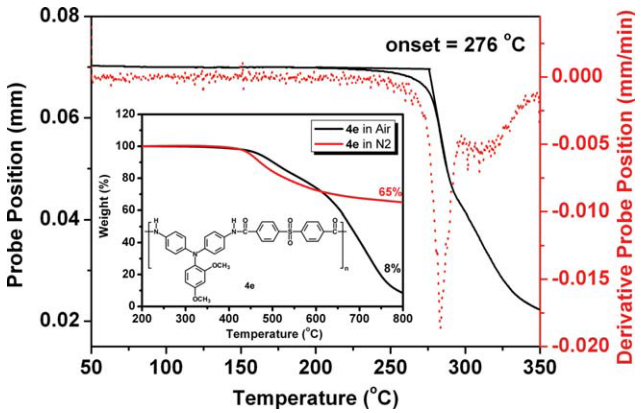

FIGURE 2 TMA and TGA curves of polyamide **4e** at a heating rate of 10 °C/min and 20 °C/min, respectively. [Color figure can be viewed in the online issue, which is available at www.interscience.wiley.com.]

TABLE 2 Optical and Electrochemical Properties of Polyamides

	In Solution[a]			As Film		Oxidation Potential (V vs. Ag/AgCl in MeCN)				HOMO[c] (eV)		LUMO[c] (eV)	
Index	λ_{max}^{Abs} (nm)	λ_{max}^{PL} (nm)	Φ_F[d] (%)	λ_{max}^{Abs} (nm)	λ_{onset}^{Abs} (nm)	$E_{1/2}$[e]	E_{pa}[f]	E_{onset}	E_g[b] (eV)	$E_{1/2}$	E_{onset}	$E_{1/2}$	E_{onset}
4a	283, 363	461	0.53	363	458	0.69 (0.73)[g] (0.87)[h]	0.80, 1.28	0.56	2.71	5.05	4.99	2.34	2.28
4b	346	449	0.77	344	427	0.69 (0.75) (0.85)	0.83, 1.31	0.56	2.90	5.05	4.99	2.15	2.09
4c	294, 361	459	0.37	359	453	0.69 (0.75) (0.86)	0.82, 1.29	0.56	2.74	5.05	4.99	2.31	2.25
4d	337	455	0.41	338	410	0.70 (0.76) (0.86)	0.82, 1.30	0.58	3.02	5.06	5.01	2.04	1.99
4e	278, 382	468	0.47	384	481	0.72 (0.78) (0.88)	0.86, 1.34	0.58	2.58	5.08	5.01	2.50	2.43
4f	352	448	0.42	350	437	0.73 (0.79) (0.88)	0.84, 1.36	0.59	2.84	5.09	5.02	2.25	2.18
4g	313	445	0.39	311	436	0.72 (0.74) (0.85)	0.86, 1.35	0.59	2.84	5.08	5.02	2.24	2.18
4h	301, 373	461	0.33	373	471	0.70 (0.77) (0.85)	0.81, 1.31	0.57	2.63	5.06	5.00	2.43	2.37

[a] Measured in NMP (1×10^{-5} mol/L).
[b] Band gap calculated by the equation: $E_g = 1240/\lambda_{onset}$ of polymer film.
[c] The HOMO energy levels were calculated from cyclic voltammetry and were referenced to ferrocene (4.8 eV). LUMO = HOMO − E_g.
[d] The quantum yield was calculated in an integrating sphere with quinine sulfate as the standard ($\Phi_F = 54.6\%$).
[e] Half-wave potential of the first oxidation redox couple.
[f] Anodic peak potentials.
[g] Data of analogous polyamides **4′** having the corresponding diacid residue as in the **4** series.
[h] Data of analogous polyamides **4″** having the corresponding diacid residue as in the **4** series.

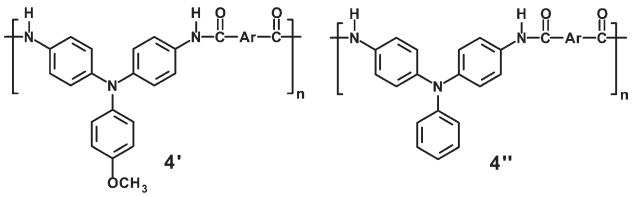

the TPA core. The second peak, at 1.30 V, can be attributed to oxidation of methoxy groups, causing radical recombination and formation of a quinoid structure (see Scheme 3). The oxidation of the polymer film of **4d** is accompanied by color changes. In the neutral state, the film is almost colorless. Applying a potential of 0.8 V, where the first oxidation takes place, the color is changed to green. If the potential is further increased to 1.3 V, where the second oxidation occurs, the color of the film turns to blue-purple. The first oxidation step is fully reversible. After 2000 oxidative cyclic scans between 0 and 1.0 V at scan rate of 100 mV/s, the polymer film still preserved superior redox reversibility (Fig. 4). However, the second oxidation process seemed to be not very reversible as that of the first one. As shown in Figure 5, the second redox wave of polymer **4d** showed a slight shift of the anodic peak and a slight decrease in current density after five cyclic scans in a potential range of 0–1.4 V at scan rate of 50 mV/s. Figure 6 compares the CV curves of structurally similar polyamides **4d**, **4d′**, and **4d″**. As expected, the onset oxidation potential of **4d** is lower as compared with those of **4d′** and **4d″** because of dimethoxy substitution on the pendent phenyl ring of the TPA unit. From polyamide **4d**, one can also observe a second oxidation process at 1.30 V, which yields a dication, whereas the corresponding **4d′** and **4d″** analogues show only a single wave. This result indicated that the presence of the second electron-donating methoxy substituent stablilizes the quinoneimine dicationic states, leading to the occurrence of the second oxidation process.

The energy levels of the highest occupied molecular orbital (HOMO) and lowest unoccupied molecular orbital (LUMO) of the investigated polyamides can be determined from the oxidation onset potentials (E_{onset}) or half-wave potentials ($E_{1/2}$) and the onset absorption wavelengths, and the results are listed in Table 2. The external ferrocene/ferrocenium (Fc/Fc^+) redox standard $E_{1/2}$ is 0.44 V versus Ag/AgCl in MeCN. Assuming that the HOMO energy for the Fc/Fc^+ standard was 4.80 eV with respect to the zero vacuum level, we can estimate the HOMO energy levels for polyamides **4a–h** to be in the range of 4.99–5.02 eV and 5.05–5.09 eV calculated from E_{onset} and $E_{1/2}$, respectively. The lower ionization

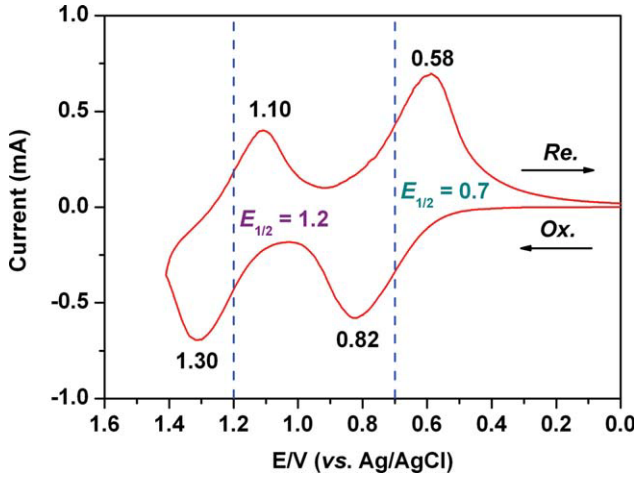

FIGURE 3 The first CV scan of the cast film of polyamide **4d** on an ITO-coated glass substrate in 0.1 M TBAP/MeCN solution (scan rate = 50 mV/s). $E_{1/2}$ values are indicated by blue dashed lines. [Color figure can be viewed in the online issue, which is available at www.interscience.wiley.com.]

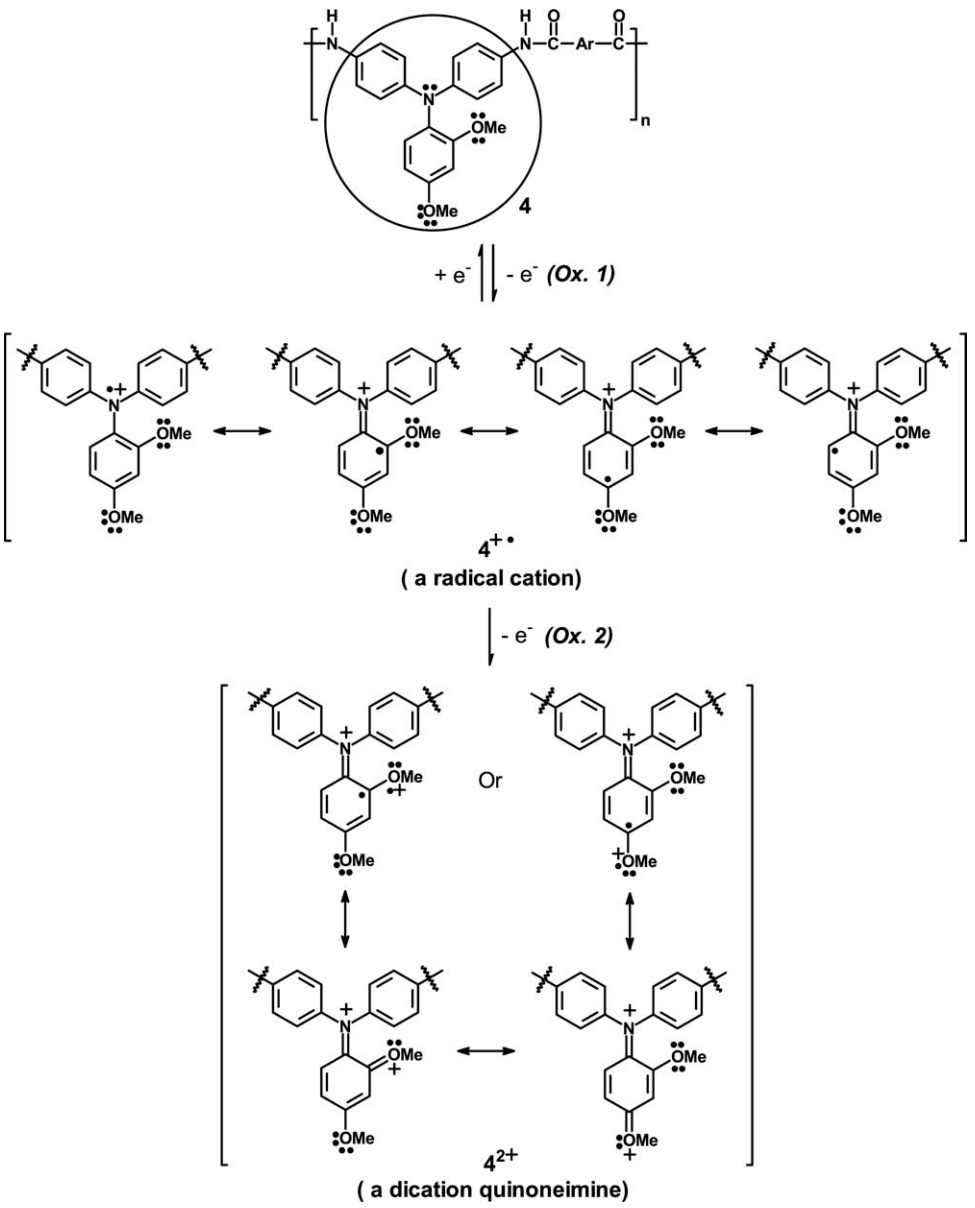

SCHEME 3 Proposed anodic oxidation pathways of the polyamides.

potential could suggest an easier hole injection into films from ITO electrodes in electronic device applications.

Spectroelectrochemical and Electrochromic Properties

The spectroelectrochemical properties of the polymer thin films were monitored by a UV–vis spectrometer at different applied potentials. The electrode preparations and solution conditions were identical to those used in CV. The typical absorption spectral changes of polyamide **4d** are shown in Figure 7. The polyamide **4d** started to be oxidized at about 0.6 V. When the applied potential was gradually raised from 0.6 to 0.8 V, the absorption intensity at 337 nm slightly dropped, while a new peak at 397 nm and a broadband having its maximum absorption wavelength at 829 nm appeared. The spectral changes were clearly due to the formation of the radical cationic states of the polyamide **4d** by electron removal from the lone pair on the nitrogen atom on the TPA unit. On this oxidized state, polyamide **4d** absorbed in the regions below 450 nm and above 550 nm with a valley (absorption minimum) at 450–550 nm, reflecting a green color. As the applied potential was adjusted to 1.1 V or above, another absorption band originated from the dicationic dimethoxyTPA moiety (see Scheme 3) showed up around 614 nm with a concomitant decrease of absorption intensity at 397 nm. These changes in electronic absorption spectra of **4d** on further oxidation were nicely reflected by color change from green to a blue-purple color. These results indicated the occurrence of a two-step oxidation sequence during the oxidation of **4d**. A similar spectral change was observed for other polyamides of this series.

The film color of polyamide **4d** turned into green and blue-purple with high contrast of optical transmittance change

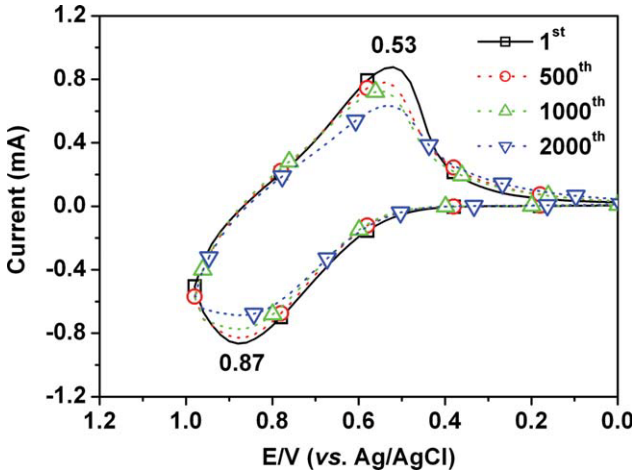

FIGURE 4 Repetitive CV scanning of the polyamide **4d** film on an ITO electrode in 0.1 M TBAP/MeCN solution over the potential range from 0 to 1.0 V at a scan rate of 100 mV/s. [Color figure can be viewed in the online issue, which is available at www.interscience.wiley.com.]

(ΔT%) up to 84% at 829 nm, 68% at 614 nm, and 54% at 397 nm as shown in Figure 7. The color switching times were estimated by applying a potential step, and the absorbance profiles were followed. The switching time was defined as the time that was required to reach 90% of the full change in absorbance after switching potential. Thin films from polymer **4d** would require 1.7 s at 0.8 V for switching absorbance at 829 nm and 1.0 s for bleaching as shown in Figure 8.

The long-term stability of the film of **4d** was determined by measuring the optical absorbance change as a function of the number of switching cycles. We extracted the electrochromic parameters of the **4d** film by analysis of transmittance change decrement or increment of the absorption band at 337, 397, and 829 nm with respect to time while the potential was switched between the neutral (−0.5 V) and the first oxidized states (+0.8 V) with a residence time of 14 s. During this measurement, % transmittance (%T) at the wavelength of maximum contrast was determined by using a UV–vis spectrophotometer. The optical contrast measured as the difference between %T at neutral and oxidized states (ΔT) were found to be 34%, 54%, and 84% for 337, 397, and 829 nm, respectively (Fig. 9). The electrochromic coloration efficiency (CE; η) can be calculated via optical density using the following equation:[27]

$$\eta = \Delta \mathrm{OD}/Q$$

where ΔOD is the optical absorbance change and Q (mC/cm^2) is the injected/ejected charge during a redox step. On the basis of this equation, the CE of polyamide **4d** was found to be 329 cm^2/C, which was higher than that of many conjugated polymers.[18] No significant change in redox response of the polymer was observed at the end of 1000 cycles. Its optical activity retained by 80% even after 1000 cycles, namely exhibits high redox stability.

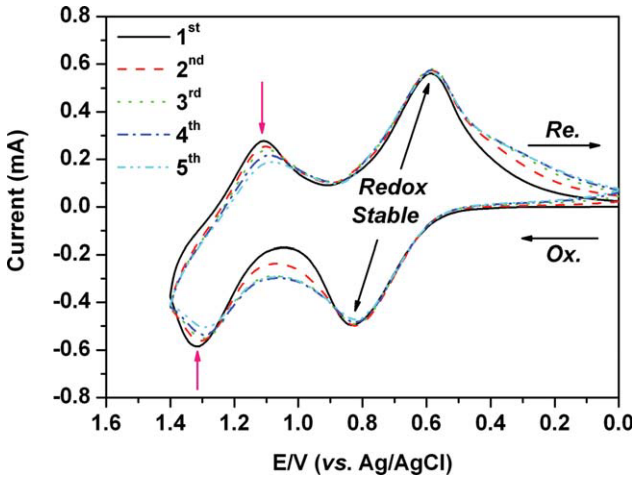

FIGURE 5 Repetitive CV scanning of the polyamide **4d** film on the ITO/glass electrode in 0.1 M TBAP/MeCN solution over the potential range from 0 to 1.5 V at a scan rate of 50 mV/s. [Color figure can be viewed in the online issue, which is available at www.interscience.wiley.com.]

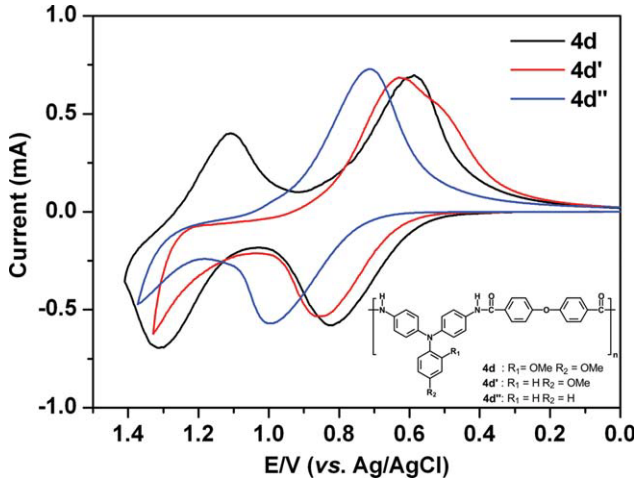

FIGURE 6 Cyclic voltammograms of the cast films of polyamides **4d**, **4d**′, and **4d**″ on an ITO-coated glass substrate in 0.1 M TBAP/MeCN solution at a scan rate of 50 mV/s. [Color figure can be viewed in the online issue, which is available at www.interscience.wiley.com.]

CONCLUSIONS

A series of new redox-active polyamides has been prepared from 4,4′-diamino-2″,4″-dimethoxytriphenylamine with various aromatic dicarboxylic acids. Incorporation of 2,4-dimethoxytriphenylamine units to the polymer main chain not only functionalizes the polyamides with stable redox properties but also leads to enhanced solubility and good thin-film formability. Aside from high T_g and T_s values and good thermal stability, the polymers also revealed stable electrochromic properties, changing color from colorless or pale yellow neutral state to green or blue-purple oxidized state. The

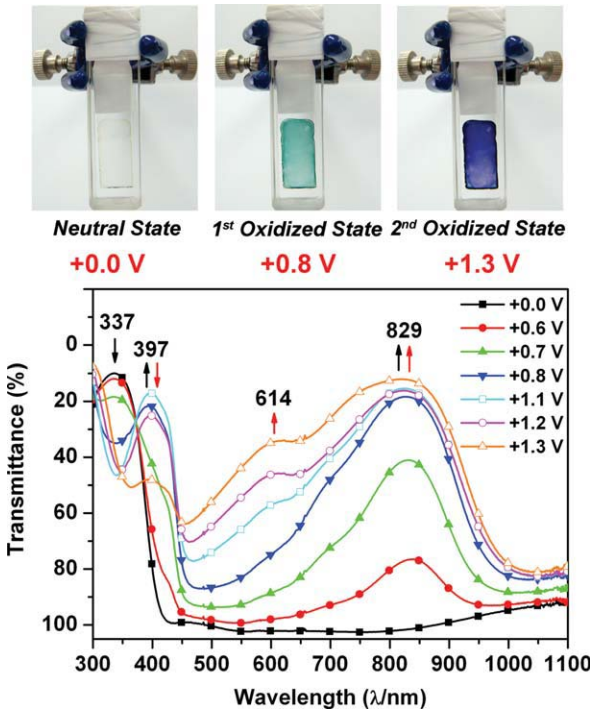

FIGURE 7 Spectroelectrochemical series of polyamide **4d** (in MeCN with 0.1 M TBAP as supporting electrolyte) at various applied potentials (vs. Ag/AgCl). The photographs show the color changes of the film in electrochemical cell at indicated electrode voltages.

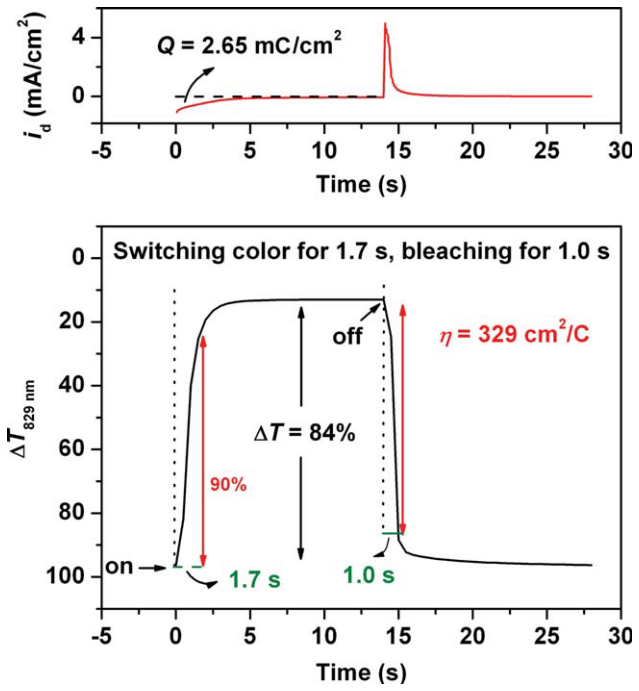

FIGURE 8 Dynamic changes of the transmittance and current upon switching the potential between −0.5 and 0.8 V (vs. Ag/AgCl) with a pulse width of 14 s applied to the cast film of polyamide **4d** on the ITO-coated glass slide in MeCN containing 0.1 M TBAP. The absorption was recorded at 829 nm.

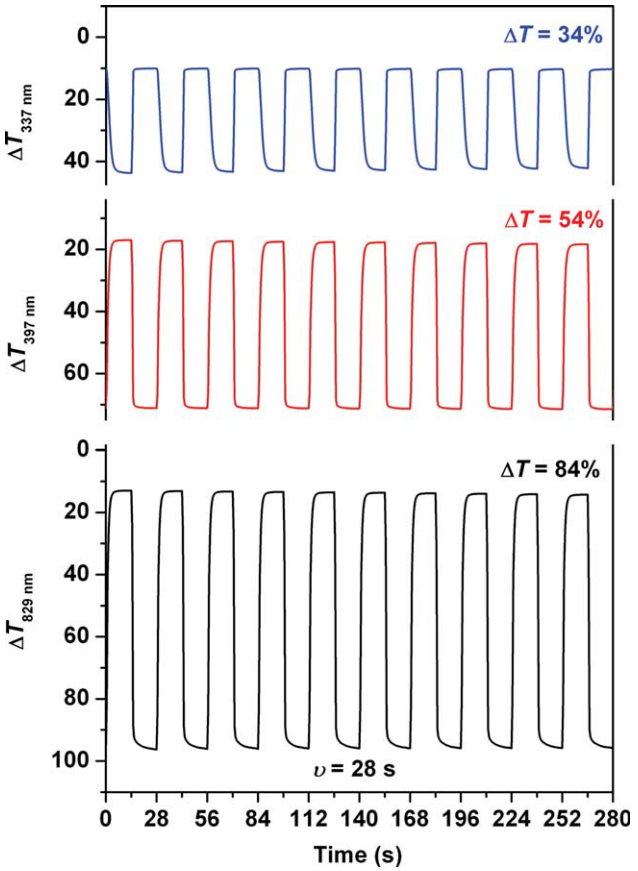

FIGURE 9 Optical transmittance changes for polyamide **4d** film on ITO-glass substrate (active area ~1 cm^2) at 337, 397, and 829 nm in 0.1 M TBAP/MeCN while the polymer was switched between −0.5 and 0.8 V with a switch time of 14 s.

polymer films exhibited high coloration efficiency, high optical contrast ratio, reasonable response times, and long-term redox and electrochromic reversibility. Thus, these polymers may find optoelectronic applications as new hole-transporting and electrochromic materials because of their proper HOMO values and stable electrochromic behavior.

The authors thank the National Science Council of Taiwan (ROC) for financial support through the research grant NSC 97-2221-E-027-113-MY3.

REFERENCES AND NOTES

1 Monk, P. M. S.; Mortimer, R. J.; Rosseinsky, D. R. Electrochromism and Electrochromic Devices; Cambridge University Press: Cambridge, UK, 2007.

2 Rauh, R. D. Electrochim Acta 1999, 44, 3165–3176.

3 Rosseinsky, D. R.; Mortimer, R. J Adv Mater 2001, 13, 783–793.

4 Heuer, H. W.; Wehrmann, R.; Kirchmeyer, S. Adv Funct Mater 2002, 12, 89–94.

5 Mortimer, R. J.; Dyer, A. L.; Reynolds, J. R. Displays 2006, 27, 2–18.

6 Sonmez, G.; Sonmez, H. B. J Mater Chem 2006, 16, 2473–2477.

7 Anderson, P.; Forchheimer, R.; Tehrani, P.; Berggren, M. Adv Funct Mater 2007, 17, 3074–3082.

8 Baetens, R.; Jelle, B. P.; Gustavsen, A. Sol Energy Mater Sol Cells 2010, 94, 87–105.

9 Beaupre, S.; Breton, A. C.; Dumas, J.; Leclerc, M. Chem Mater 2009, 21, 1504–1513.

10 (a) Dautremont-Smith, W. C.; Displays 1982, 3, 3–22; (b) Dautremont-Smith, W. C. Displays 1982, 3, 67–80.

11 Niklasson, G. A.; Granqvist, C. G. J Mater Chem 2007, 17, 127–156.

12 (a) Mortimer, R. J Chem Soc Rev 1997, 26, 147–156; (b) Mortimer, R. J. Electrochim Acta 1999, 44, 2971–2981; (c) Rowley, N. M.; Mortimer, R. J. Sci Prog 2002, 85, 243–262.

13 Sonmez, G. Chem Commun 2005, 5251–5259.

14 Beaujuge, P. M.; Reynolds, J. R. Chem Rev 2010, 110, 268–320.

15 Patra, A.; Bendikov, M. J Mater Chem 2010, 20, 422–433.

16 (a) Groenendaal, L.; Zotti, G.; Aubert, P. H.; Waybright, S. M.; Reynolds, J. R. Adv Mater 2003, 15, 855–879; (b) Walczak, R. M.; Reynolds, J. R. Adv Mater 2006, 18, 1121–1131; (c) Beaujuge, P. M.; Ellinger, S.; Reynolds, J. R. Nat Mater 2008, 7, 795–799; (d) Beaujuge, P. M.; Ellinger, S.; Reynolds, J. R. Adv Mater 2008, 20, 2772–2776; (e) Unur, E.; Beaujuge, P. M.; Ellinger, S.; Jung, J.-H.; Reynolds, J. R. Chem Mater 2009, 21, 5145–5153; (f) Amb, C. M.; Beaujuge, P. M.; Reynolds, J. R. Adv Mater 2010, 22, 724–728.

17 (a) Sonmez, G.; Meng, H.; Wudl, F. Chem Mater 2004, 16, 574–580; (b) Sonmez, G.; Sonmez, H. B.; Shen, C. K. F.; Jost, R. W.; Rubin, Y.; Wudl, F. Macromolecules 2005, 38, 669–675.

18 (a) Ko, H. C.; Kim, S.; Lee, H.; Moon, B. Adv Funct Mater 2005, 15, 905–909; (b) Wu, C. G.; Lu, M. I.; Chang, S. J.; Wei, C. S. Adv Funct Mater 2007, 17, 1063–1070; (c) Balan, A.; Gunbas, G. E.; Durmus, A.; Toppare, L. Chem Mater 2008, 20, 7510–7513; (d) Cihaner, A.; Algi, F. Adv Funct Mater 2008, 18, 3583–3589; (e) Koyuncu, S.; Zafer, C.; Sefer, E.; Koyuncu, F. B.; Demic, S.; Kaya, I.; Ozdemir, E.; Icli, S. Synth Met 2009, 159, 2013–2021; (f) Pamuk, M.; Tirkes, S.; Cihaner, A.; Algi, F. Polymer 2010, 51, 62–68.

19 Garcia, J. M.; Garcia, F. C.; Serna, F.; de la Pena, J. L. Prog Polym Sci 2010, 35, 623–686.

20 (a) Espeso, J. F.; de la Campa, J. G.; Lozano, A. E.; de Abajo, J. J Polym Sci Part A: Polym Chem 2000, 38, 1014–1023; (b) Espeso, J. F.; Ferrero, E.; de la Campa, J. G.; Lozano, A. E.; de Abajo, J. J Polym Sci Part A: Polym Chem 2001, 39, 475–485; (c) Ferreiro, J. J.; de la Campa, J. G.; Lozano, A. E.; de Abajo J. J Polym Sci Part A: Polym Chem 2005, 43, 5300–5311; (d) Espeso, J. F.; Lozano, A. E.; de la Campa, J. G.; Garcia-Yoldi, I.; de Abajo, J. J Polym Sci Part A: Polym Chem 2010, 48, 1743–1751.

21 (a) Hsiao, S.-H.; Huang, T.-L. J Polym Sci Part A: Polym Chem 2002, 40, 947–957; (b) Liou, G.-S.; Hsiao, S.-H. J Polym Sci Part A: Polym Chem 2002, 40, 1781–1789; (c) Wu, S.-C.; Shu, C.-F. J Polym Sci Part A: Polym Chem 2003, 41, 1160–1166; (d) Hsiao, S.-H.; Chang, Y.-M. J Polym Sci Part A: Polym Chem 2004, 42, 4056–4062; (e) Su, T.-H.; Hsiao, S.-H.; Liou, G.-S. J Polym Sci Part A: Polym Chem 2005, 43, 2085–2098.

22 (a) Liou, G.-S.; Hsiao, S.-H.; Ishida, M.; Kakimoto, M.; Imai, Y. J Polym Sci Part A: Polym Chem 2002, 40, 2810–2818; (b) Liou, G.-S.; Hsiao, S.-H. J Polym Sci Part A: Polym Chem 2003, 41, 94–105.

23 (a) Cheng, S.-H.; Hsiao, S.-H.; Su, T.-H.; Liou, G.-S. Macromolecules 2005, 38, 307–316; (b) Liou, G.-S.; Huang, N.-K.; Yang, Y.-L. J Polym Sci Part A: Polym Chem 2006, 44, 4059–4107; (c) Hsiao, S.-H.; Chang, Y.-M.; Chen, H.-W.; Liou, G.-S. J Polym Sci Part A: Polym Chem 2006, 44, 4579–4592; (d) Liou, G.-S.; Hsiao, S.-H.; Huang, N.-K.; Yang, Y.-L. Macromolecules 2006, 39, 5337–5346; (e) Chang, C.-W.; Liou, G.-S.; Hsiao, S.-H. J Mater Chem 2007, 17, 1007–1015; (f) Hsiao, S.-H.; Liou, G.-S.; Kung, Y.-C.; Yen, H.-J. Macromolecules 2008, 41, 2800–2808; (g) Chang, C.-W.; Liou, G.-S. J Mater Chem 2008, 18, 5638–5646; (h) Yen, H.-J.; Liou, G.-S. J Polym Sci Part A: Polym Chem 2008, 46, 7354–7368; (i) Chang, C.-W.; Yen, H.-J.; Huang, K.-Y.; Yeh, J.-M.; Liou, G.-S. J Polym Sci Part A: Polym Chem 2008, 46, 7937–7949; (j) Lin, H.-Y.; Liou, G.-S. J Polym Sci Part A: Polym Chem 2009, 47, 285–294; (k) Kung, Y.-C.; Liou, G.-S.; Hsiao, S.-H. J Polym Sci Part A: Polym Chem 2009, 47, 1740–1755; (l) Liou, G.-S.; Lin, K.-H. J Polym Sci Part A: Polym Chem 2009, 47, 1988–2001; (m) Liou, G.-S.; Chang, H.-W.; Lin, K.-H.; Su, Y. O. J Polym Sci Part A: Polym Chem 2009, 47, 2118–2131; (n) Hsiao, S.-H.; Liou, G.-S.; Wang, H.-M. J Polym Sci Part A: Polym Chem 2009, 47, 2330–2343; (o) Chang, H.-W.; Lin, K.-H.; Chueh, C.-C.; Liou, G.-S.; Chen, W.-C. J Polym Sci Part A: Polym Chem 2009, 47, 4037–4050; (p) Yen, H.-J.; Liou, G.-S. Chem Mater 2009, 21, 4062–4070.

24 (a) Seo, E. T.; Nelson, R. F.; Fritsch, J. M.; Marcoux, L. S.; Leedy, D. W.; Adams, R. N. J Am Chem Soc 1966, 88, 3498–3503; (b) Nelson, R. F.; Adams, R. N. J Am Chem Soc 1968, 90, 3925–3930; (c) Zhao, H.; Tanjutco, C.; Thayumanavan, S. Tetrahedron Lett 2001, 42, 4421–4424; (d) Selby, T. D.; Kim, K. Y.; Blackstock, S. C. Chem Mater 2002, 14, 1685–1690; (e) Amthor, S.; Noller, B.; Lambert, C. Chem Phys 2005, 316, 141–152.

25 Oishi, Y.; Takado, H.; Yoneyama, M.; Kakimoto, M.; Imai, Y. J Polym Sci Part A: Polym Chem 1990, 28, 1763–1769.

26 (a) Yamazaki, N.; Higashi, F.; Kawabata, J. J Polym Sci Polym Chem Ed 1974, 12, 2149–2155; (b) Yamazaki, N.; Matsumoto, M.; Higashi, F. J Polym Sci Polym Chem Ed 1975, 13, 1373–1380.

27 Mortimer, R. J.; Reynolds, J. R. J Mater Chem 2005, 15, 2226–2233.